

HESS J1731-347 and the existence of exotic matter: Kaon condensation in neutron stars

Polychronis Koliogiannis^{1,2,}, Vlasios Petousis³, Martin Veselský³, and Charalampos Moustakidis²*

¹Department of Physics, Faculty of Science, University of Zagreb, Bijenička cesta 32, 10000 Zagreb, Croatia

²Department of Theoretical Physics, Aristotle University of Thessaloniki, Thessaloniki, 54124, Greece

³Institute of Experimental and Applied Physics, Czech Technical University, Prague, 110 00, Czechia

Abstract. The recent observation of a compact star with the lowest observable mass of $0.77^{+0.20}_{-0.17} M_{\odot}$ within the supernova remnant HESS J1731-347 has redefined our understanding for the dense nuclear matter equation of state and enhances the existence of exotic matter. In the present work, we investigate the possible existence of kaon condensation in hadronic neutron stars through the framework of the Momentum-Dependent Interaction nuclear model describing the dense nuclear matter. We concentrate on the strangeness content of the proton and its implications on both the microscopic and macroscopic properties of neutron stars. The aforementioned quantity is of interest as it is also directly related to the location of the phase transition to kaons. The simultaneous description of the compact object within the HESS J1731-347 and the maximum observable neutron star mass imposes severe constraints on the strangeness content of the proton and the critical density for kaon condensation. The present study along with observations of neutron stars, may help to provide tighter constraints on the equation of state of dense nuclear matter and, even more, to shed light to the existence of an exotic core in neutron stars.

1 Introduction

Neutron stars are formed as a result of a supernova core-collapse and represent a fascinating end state for massive stars [1]. These stars are the most compact stars in the universe with internal hadronic structure and provide an excellent extraterrestrial laboratory for the physics of supercondensed matter. Since the outer crust of neutron stars is well-established, the interest is focused on the inner core, where many phase transitions may occur in superdense matter. The aforementioned possible new phases could be hyperons, a mixed phase of hyperons and quarks, quarks, and a boson condensate [1–6].

The constitution of the inner core of a neutron star depends explicitly on the equation of state (EoS) which remains unknown considering both the theoretical and experimental predictions. Since neutron stars resemble an extension of finite nuclei, the low density region consists mainly of hadrons (neutrons and protons), with additional contributions from leptons (electrons and muons). However, at high densities, the behavior of neutron star matter is subjected to many speculations. In this region, one possible procedure is the strangeness process in the form of a boson condensate, such as pions or kaons [2, 3]. In the pioneering work of Kaplan and Nelson [7], the authors suggested that the strong interaction of negatively charged kaons with the nuclear medium, may sufficiently reduce their effective mass in a way that bosons may replace electrons as the neutralizing agent in charge neutral matter. The charge neutrality condition in neutron stars favors a kaon

condensation because the neutrons at the top of the Fermi sea decay into protons and electrons. As a result, when the electron chemical potential matches the effective kaon mass, the kaons appear into the zero momentum state for conserving the charge neutrality.

In the present study, we investigate the possible phase transition from hadronic matter to a phase that contains baryons and kaon condensation by utilizing the well-established Momentum-Dependent Interaction (MDI) nuclear model [8]. The strong interactions due to a kaon condensation are moderated by the strangeness content of the proton. In this argument, we focus on the role of the strangeness content of the proton (protons consist of valence quarks that are confined and exist in a sea of quark-antiquark pairs, with survival probability reaching a maximum of 33%, while always strangeness quantum number remains zero) along with its consequences on both microscopic, such as the baryon density, the proton fraction, and the speed of sound, and macroscopic properties, such as the gravitational mass and the corresponding radius, of neutron stars. In addition, we emphasize to the relation between the threshold density for the appearance of kaons and the strangeness content of the proton. Finally, we devote a part for the description of the ultralight compact object within the supernova remnant HESS J1731-347, specifically considering a neutron star with the onset of kaon condensation.

The paper is structured as follows. Section 2 provides the theoretical framework for the MDI model, emphasizing the kaons interaction, while Section 3 displays the results of the present study and discusses their implications. Finally, Section 4 contains the scientific remarks.

*e-mail: pkoliogi@auth.gr

2 Theoretical Framework

2.1 β -equilibrated matter

The starting point for a system that includes kaons, nucleons, electrons and muons is to define the ground state. Nuclear matter in order to be stable at high densities must be in a chemical equilibrium for all reactions. In general, both β -decay and inverse β -decay would take place as [3, 6]

$$n \rightarrow p + e^- + \bar{\nu}_e, \quad p + e^- \rightarrow n + \nu_e. \quad (1)$$

By assuming cold neutron star matter, neutrinos have left the system leading to

$$\mu_n - \mu_p = \mu_e, \quad (2)$$

where μ_n , μ_p and μ_e are the chemical potentials of neutrons, protons and electrons, respectively. Furthermore, when the electron Fermi energy is greater than the muon mass, it is energetically favorable for electrons to decay into muons and be in a chemical equilibrium state

$$e^- \rightarrow \mu^- + \bar{\nu}_\mu + \nu_e, \quad \mu_\mu = \mu_e. \quad (3)$$

If the negatively charged kaon effective mass is sufficiently low in dense matter, then the following strangeness processes take place

$$n \leftrightarrow p + K^-, \quad e^- \leftrightarrow K^- + \nu_e, \quad (4)$$

and by assuming that the aforementioned processes take place fast enough to establish chemical equilibrium, the chemical potentials can be described as

$$\mu_n - \mu_p = \mu, \quad \mu_e = \mu, \quad (5)$$

where μ is the chemical potential of the negatively charged kaon condensate.

2.2 MDI model - Fixed baryon number state

For the description of the neutron star matter properties we employed the model introduced by Kaplan and Nelson [7] and include nuclear interactions according to the work of Thorsson et al. [3]. In particular, the calculation of the effective energy density of the neutron star matter for a fixed baryon number state is defined as [3]

$$\begin{aligned} \tilde{\mathcal{E}}(u, x, \mu, \theta) = & \mathcal{E}_{\text{MDI}}(u, x = 1/2) + u\rho_0(1 - 2x)^2 S(u) \\ & - f^2 \frac{\mu^2}{2(\hbar c)^3} \sin^2 \theta + f^2 \frac{2m_K^2 c^4}{(\hbar c)^3} \sin^2 \frac{\theta}{2} \\ & + \mu u \rho_0 x - \mu u \rho_0 (1 + x) \sin^2 \frac{\theta}{2} \\ & + (2a_1 m_s x + 2a_2 m_s + 4a_3 m_s) u \rho_0 \sin^2 \frac{\theta}{2} \\ & + \tilde{\mathcal{E}}_e + \eta(|\mu| - m_\mu c^2) \tilde{\mathcal{E}}_\mu, \end{aligned} \quad (6)$$

where ρ_0 is the nuclear saturation density, $u = \rho/\rho_0$ is the nucleon density ratio, $\mathcal{E}_{\text{MDI}}(u, x = 1/2)$ is the energy density of symmetric nuclear matter defined through the MDI model [8], $S(u)$ is the nuclear symmetry energy, x is the

proton fraction, μ is the chemical potential, θ is an amplitude parameter for the appearance of kaons, $f = 93$ MeV is the pion decay constant, m_K is the mass of the negatively charged kaon, and the constants $a_1 m_s$ and $a_2 m_s$ are equal to -67 MeV and 134 MeV, respectively. As far as concerning the coefficient $a_3 m_s$, there is a large uncertainty for its value that is related to the strangeness content of the proton. Precisely, the $a_3 m_s$ takes values in the range $[-134, -310]$ MeV corresponding to $[0\%, 20\%]$, respectively [3]. In the present work we employed the values $a_3 m_s = [-134, -222, -230, -240, -250, -260, -270, -280, -290]$ MeV. The $\eta(x)$ function is a Heaviside function related to the appearance of muons. The contribution due to leptons (electrons and muons) are given by

$$\tilde{\mathcal{E}}_e = -\frac{\mu^4}{12\pi^2(\hbar c)^3}, \quad (7)$$

$$\begin{aligned} \tilde{\mathcal{E}}_\mu = & \frac{m_\mu^4 c^8}{8\pi^2(\hbar c)^3} \left[(2t^2 + 1) t \sqrt{t^2 + 1} - \ln(t + \sqrt{t^2 + 1}) \right] \\ & - \mu \frac{p_{F_\mu}^3}{3\pi^2(\hbar c)^3}, \end{aligned} \quad (8)$$

where $p_{F_\mu} = \sqrt{\mu^2 - m_\mu^2 c^4}$ is the muon Fermi momentum and $t = p_{F_\mu}/(m_\mu c^2)$.

To define the energy density of the charge neutral ground state, we calculated the ground state of the effective energy density [3]. Specifically, we extremizing the effective energy density for a fixed baryon state with respect to the proton fraction, the chemical potential, and the amplitude

$$\begin{aligned} \frac{\partial \tilde{\mathcal{E}}}{\partial x} : & \mu - 4(1 - 2x)S(u) \sec^2 \frac{\theta}{2} + 2a_1 m_s \tan^2 \frac{\theta}{2} = 0, \\ \frac{\partial \tilde{\mathcal{E}}}{\partial \mu} : & \frac{f^2 \mu}{(\hbar c)^3} \sin^2 \theta + u \rho_0 (1 + x) \sin^2 \frac{\theta}{2} - x u \rho_0 + \frac{\mu^3}{3\pi^2(\hbar c)^3} \\ & + \eta(|\mu| - m_\mu c^2) \frac{(\mu^2 - m_\mu^2 c^4)^{3/2}}{3\pi^2(\hbar c)^3} = 0, \\ \frac{\partial \tilde{\mathcal{E}}}{\partial \theta} : & \cos \theta - \frac{1}{\mu^2} \left(m_K^2 c^4 - \frac{(\hbar c)^3 \mu}{2f^2} u \rho_0 (1 + x) \right. \\ & \left. + \frac{(\hbar c)^3 u \rho_0}{2f^2} (2a_1 x + 2a_2 + 4a_3) m_s \right) = 0. \end{aligned} \quad (9)$$

2.3 Equation of State

The energy density for the construction of the EoS is given by the relation [3]

$$\begin{aligned} \mathcal{E}(u, x, \mu, \theta) = & \mathcal{E}_{\text{MDI}}(u, x = 1/2) + u \rho_0 (1 - 2x)^2 S(u) \\ & + f^2 \frac{\mu^2}{2(\hbar c)^3} \sin^2 \theta + f^2 \frac{2m_K^2 c^4}{(\hbar c)^3} \sin^2 \frac{\theta}{2} \\ & + (2a_1 m_s x + 2a_2 m_s + 4a_3 m_s) u \rho_0 \sin^2 \frac{\theta}{2} \\ & + \mathcal{E}_e + \eta(|\mu| - m_\mu c^2) \mathcal{E}_\mu, \end{aligned} \quad (10)$$

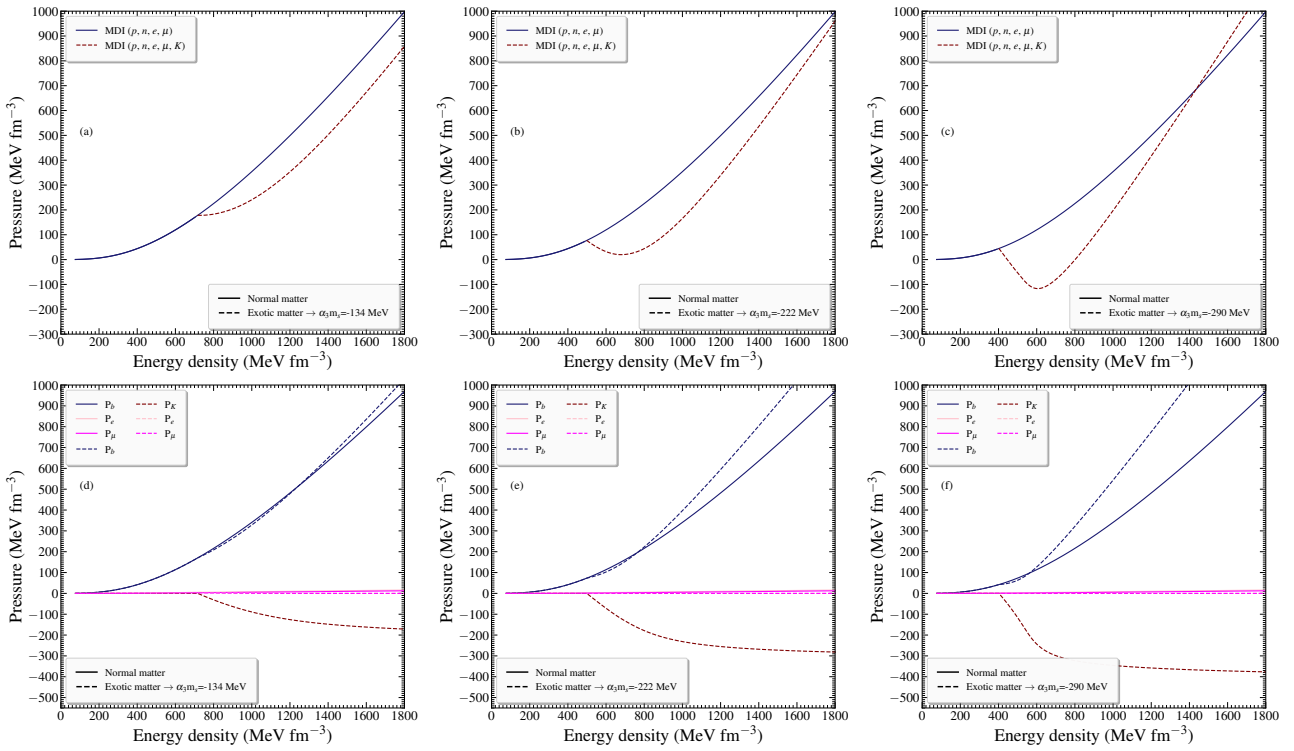


Figure 1. (a-c) Pressure as a function of the energy density for the MDI-80 EoS with a_{3m_s} equal to $[-134, -222, -290]$ MeV. The normal matter is presented with the solid line, while the exotic matter with the dashed line. (d-f) Pressure contribution as a function of the energy density for the MDI-80 EoS with a_{3m_s} equal to $[-134, -222, -290]$ MeV. The contribution of particles to normal matter is presented with the solid lines, while the contribution of particles to exotic matter with the dashed lines.

where

$$\mathcal{E}_e = \frac{\mu^4}{4\pi^2(\hbar c)^3}, \quad (11)$$

$$\mathcal{E}_\mu = \frac{m_\mu^4 c^8}{8\pi^2(\hbar c)^3} \left[(2t^2 + 1)t \sqrt{t^2 + 1} - \ln(t + \sqrt{t^2 + 1}) \right], \quad (12)$$

and the pressure is given by the relation [9]

$$p(u, x, \mu, \theta) = p_b(u, x) + p_K(\mu, \theta) + p_e + \eta(|\mu| - m_\mu c^2)p_\mu, \quad (13)$$

where

$$\begin{aligned} p_b(u, x) &= u^2 \frac{\partial}{\partial u} \left(\frac{\mathcal{E}_b(u, x)}{u} \right), \\ p_K(\mu, \theta) &= -f^2 \frac{\mu^2}{2(\hbar c)^3} \sin^2 \theta - f^2 \frac{2m_K^2 c^4}{(\hbar c)^3} \sin^2 \frac{\theta}{2}, \\ p_{l=e,\mu} &= \frac{m_l^4 c^5}{24\pi^2 \hbar^3} \left[(2z^3 - 3z)(1 + z^2)^{1/2} + 3 \sinh^{-1} z \right], \end{aligned} \quad (14)$$

with $z = (\hbar c) (3\pi^2 \rho x_l)^{1/3} (m_l c^2)^{-1}$.

3 Results and Implications

3.1 Pressure - Energy relations

In the present work, we employed the parametrization for the MDI-80 model regarding the hadronic matter. In par-

ticular, the MDI-80 model corresponds to slope parameter $L_0 = 80$ MeV, symmetry energy $S_0 = 32$ MeV and incompressibility $K_0 = 240$ MeV at the saturation density. It needs to be mentioned that since the main purpose of the paper is to study the effect of the strangeness content of the proton on the EoS alongside the ultralight compact object within the supernova remnant HESS J1731-347 through the kaon condensation, we presented only one EoS. Similar results are produced for a wide range of EoSs based on the MDI model.

Figure 1 (a-c) displays the pressure as a function of the energy density for the MDI-80 EoS. In particular, we present the normal matter EoS and three EoSs with a_{3m_s} equal to $[-134, -222, -290]$ MeV. It needs to be noted that as values higher than $a_{3m_s} \simeq -290$ MeV lead to EoSs with no part including kaons under the causality limit, the upper limit for the a_{3m_s} for the specific EoS is equal to -290 MeV. It is clear that as the content of the strangeness of the proton increases, the threshold density for the appearance of kaons decreases. The results also indicate that the transition from normal matter to a matter that contains kaons is of second order. However, as depicted in Figure 1 (a-c), an increase in the strangeness content of the proton beyond 0% results in a rapid decrease in pressure, even reaching negative values in some instances, following the threshold value. This reduction becomes increasingly significant as the content of the strangeness of the proton increases. Since the condensation is so strong in neutron stars, we employed a Maxwell construction (MC) [10] at

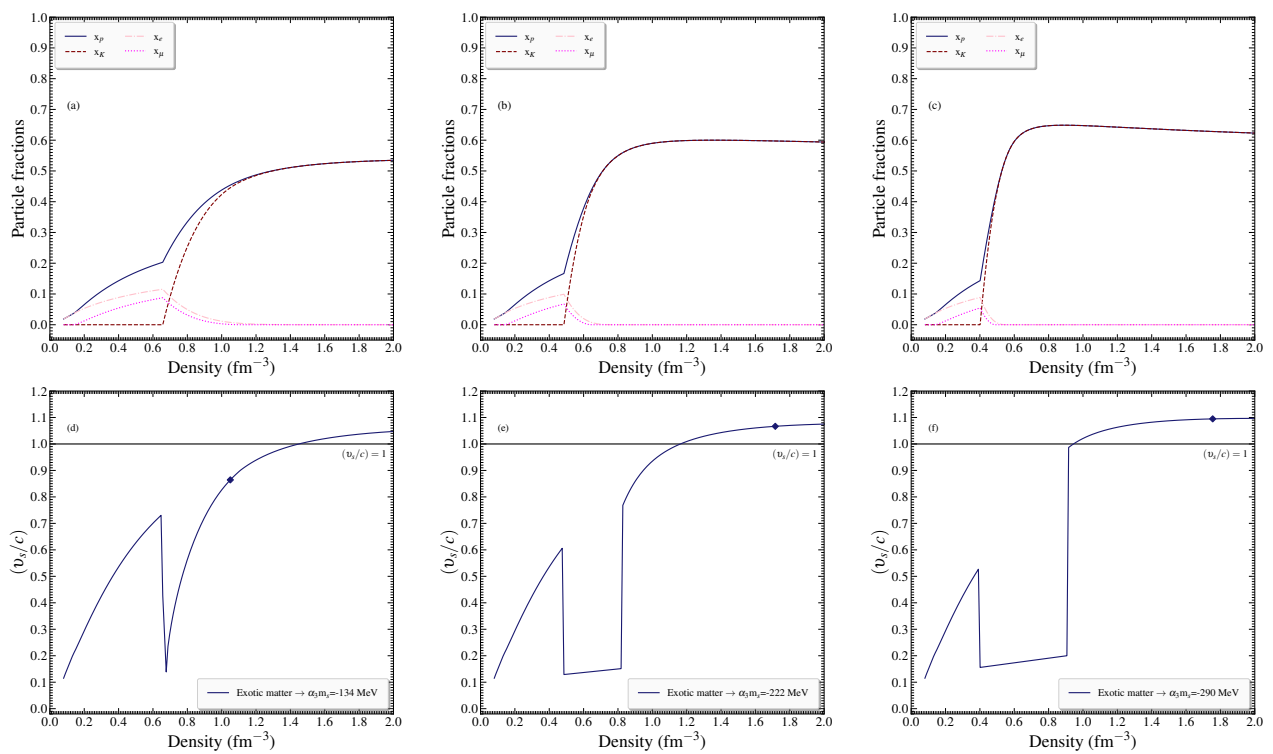


Figure 2. (a-c) Particle fractions and (d-f) speed of sound in units of speed of light as a function of the baryon density for the MDI-80 EoS with $a_3 m_s$ equal to $[-134, -222, -290]$ MeV. Diamonds indicate the maximum mass configuration. The causality limit of $(v_s/c) = 1$ is also marked to guide the eye.

the threshold value for the existence of a single value chemical potential.

In order to perceive the alter in the pressure of the EoS due to the existence of a kaon condensate, we present in Figure 1 (d-f) the contribution of baryons, kaons and leptons to the pressure. In all cases, the contribution of leptons to the total pressure is negligible both in normal and in exotic matter. However, in the case of baryons, a dramatic change occurs. As the strangeness content of the proton increases, the pressure of the baryons rises, accompanied by a corresponding decrease in the pressure of the kaons. The latter is consistent with stronger interactions that manifest as the strangeness content of the proton increases.

3.2 Proton fraction and speed of sound

A significant microscopic property related to the structure of neutron stars is the proton fraction, as well as the fractions of the rest particles throughout the process of β -equilibrium. Figure 2 (a-c) displays the fractions of the particles as a function of the baryon density for $a_3 m_s$ equal to $[-134, -222, -290]$ MeV. Prior to the condensation all the fractions are an increasing function of the density. With the onset of the condensation, the net negative charge in the kaon fields leads to a reduction in lepton concentrations, potentially causing them to vanish [3].

In addition, another quantity of great interest is the speed of sound, which must not exceed the causality limit at least up to densities that correspond to maximum mass configuration. In Figure 2 (d-f) we present the speed of

sound in units of speed of light as a function of the baryon density for $a_3 m_s$ equal to $[-134, -222, -290]$ MeV. Except for the $a_3 m_s = -134$ MeV, the rest cases exceed the causality limit before reaching the maximum mass configuration. To address this behavior, we employed a MC at a specific density value lower than those exceeding the causality limit, specifically the density where $(v_s/c) = 1$. Subsequently, we introduced the maximally stiff EoS with $(v_s/c) = 1$ beyond that density threshold. The aforementioned treatment has a negligible effect on the maximum gravitational mass configuration.

In Figure 3 we display a representative case of the speed of sound in units of speed of light as a function of the pressure for the MDI-80 EoS and the MDI-80 EoS with $a_3 m_s = -260$ MeV alongside the MC. Figure 3 features the differences in the speed of sound as the maximally stiff EoS is introduced after a specific value of baryon density or pressure (similar behavior is presented throughout the range of EoSs).

3.3 Mass-Radius relation

In Figure 4 we display the gravitational mass as a function of the equatorial radius for the normal MDI-80 EoS and the exotic ones with $a_3 m_s$ equal to $[-134, -222, -230, -240, -250, -260, -270, -280, -290]$ MeV. The kaon condensation presents a strong softening on the EoS by reducing its maximum mass up to 17.5%. However, since the main objective of this study is to provide a possible explanation of

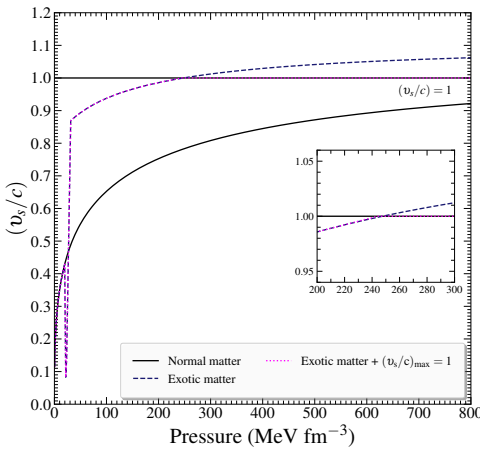


Figure 3. Speed of sound in units of speed of light as a function of the pressure for the MDI-80 EoS and the MDI-80 EoS with $a_3 m_s = -260$ MeV. The normal matter is depicted by the solid line, whereas the EoS with exotic matter is presented by the dashed line. The configuration with a fixed maximum speed of sound is denoted by the dotted line. The causality limit of $(v_s/c) = 1$ is also marked for reference.

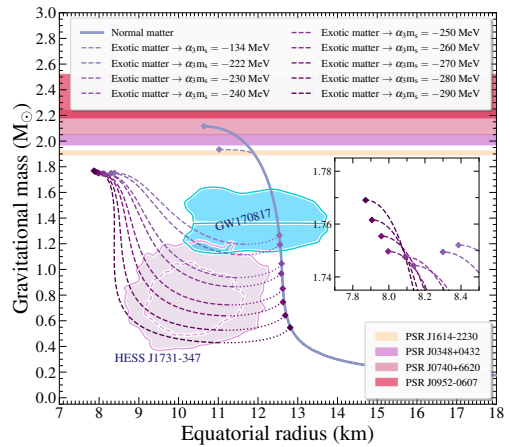


Figure 4. Gravitational mass as a function of the equatorial radius for the MDI-80 EoS. The EoS with normal matter is presented by the solid line, while the ones with exotic matter are denoted by the dashed lines. Diamonds indicate the maximum mass configurations. The shaded regions from bottom to top represent the HESS J1731-347 remnant [16], the GW170817 event [11], and the PSR J1614-2230 [12], PSR J0348+0432 [13], PSR J0740+6620 [14], and PSR J0952-0607 [15] pulsar observations with possible maximum neutron star mass.

the ultralight compact object within the supernova remnant HESS J1731-347 through a phase transition to a kaon condensate, we only focused on the cases with $a_3 m_s = [-222, -230, -240, -250, -260, -270, -280, -290]$ MeV. These scenarios are possible to describe the low mass and radius of this compact object. Thus, we provided parametrizations based on the speed of sound alongside the MC to achieve a suitable EoS that never exceeds the causality limit and aligns with the boundaries of astrophysical observations.

Figure 4 illustrates that the values $a_3 m_s = -222$ MeV and $a_3 m_s = -290$ MeV serve as boundary conditions for the ultralight compact object within the supernova remnant HESS J1731-347. The first two cases, specifically $a_3 m_s = [-222, -230]$ MeV, are capable of describing, at least marginally, the compact object and satisfying the constraints imposed by the GW170817 event [11]. The remaining cases can only account for the ultralight compact object. However, the intermediate values, $a_3 m_s = [-240, -250, -260, -270, -280]$ MeV, offer the most appropriate explanation for the ultralight compact object within the supernova remnant HESS J1731-347. Furthermore, it is notable that as the strangeness content of the proton increases, the density at which a kaon condensation occurs decreases, leading to stronger softening on the EoS. Ultimately, Figure 4 indicates that a kaon condensation could explain the ultralight compact object within the supernova remnant HESS J1731-347. However, this hypothesis presents a significant drawback, as it fails to meet the maximum mass observational constraints [12–15]. Nonetheless, further efforts are in order to address this issue.

4 Remarks

The high density behavior of the nuclear matter and the existence of many phases in the superdense matter is an open problem in nuclear astrophysics. Hence, we investigated within the MDI model the consequences of a kaon condensation into a zero momentum state in neutron stars and connect them to astrophysical observations. Specifically, we constructed EoSs by introducing various values of the strangeness content of the proton and explored their implications on neutron stars.

In kaon condensation, the strangeness content of the proton plays a significant role in determining the threshold value. Beyond this threshold, kaon condensation occurs. In particular, higher values of the strangeness content of the proton lead to lower values for the threshold density in neutron matter. The ensuing result is that the appearance of a new state of matter is taking place at lower values of baryon density in neutron stars, leading to a strong softening on the EoS.

In addition, the speed of sound presents an interesting behavior with the onset of a kaon condensation. Increasing values of the strangeness content of the proton result in exceeding the causality limit at lower values of baryon density or pressure. The latter prevents the consistent way to locate the maximum mass configuration. However, the MC to a maximally stiff EoS that introduced to address this issue, has a negligible effect on the maximum mass configuration. Thus, the MC addresses the drawback of the aforementioned behavior without interacting with the maximum mass configuration.

Furthermore, we investigated the possible explanation of the ultralight compact object within the supernova remnant HESS J1731-347 [16] which has the lowest observ-

able mass of $0.77^{+0.20}_{-0.17} M_{\odot}$ and corresponding radius of $10.4^{+0.86}_{-0.78}$ km. The main conjecture was that the appearance of a kaon condensation in dense nuclear matter would be able to soften the hadronic EoS appropriately to describe the aforementioned compact object. In fact, we concluded that for strangeness of the order of 15.5% up to 19% in the proton, the kaon condensation leads to a strong softening on the EoS, providing a suitable description for neutron stars considering the remnant. It should be emphasized that for strangeness of the order of 10% to 15% in the proton, the kaon condensation describes both the ultralight compact object with the remnant HESS J1731-347 and the astrophysical observations associated with the GW170817 event. Conversely, the existence of a kaon condensation prevents the EoS to fulfill the current observational astrophysical limits for the maximum mass [12–15]. Consequently, although the kaon condensation is a possible explanation of the remnant, there is an open problem with the maximum mass.

Future efforts should focus on the appearance of kaon or pion condensation in dense matter, incorporating various nuclear models and employing the Gibbs construction in addition to the MC. Moreover, special attention should also be given to the maximum mass. Finally, similar observations such as the HESS J1731-347, along with the observational astrophysical quantities and the microscopic properties of finite nuclei from terrestrial experiments, will provide valuable insights into the origin and appearance of a phase transition in the dense nuclear matter.

5 Acknowledgment

This work was supported by the Croatian Science Foundation under the project number HRZZ-MOBDOL-12-2023-6026, by the Croatian Science Foundation under the project number IP-2022-10-7773 and by the Czech Science Foundation (GACR Contract No. 21-24281S).

References

- [1] D. Menezes, P. Panda, C. Providencia, Kaon condensation in the quark-meson coupling model and compact stars., *Phys. Rev. C* **72**, 035802 (2005). <https://doi.org/10.1103/PhysRevC.72.035802>
- [2] G. Brown, K. Kubodera, M. Rho, V. Thorsson, A novel mechanism for kaon condensation in neutron star matter, *Phys. Lett. B* **291**, 355 (1992). [https://doi.org/10.1016/0370-2693\(92\)91386-N](https://doi.org/10.1016/0370-2693(92)91386-N)
- [3] V. Thorsson, M. Prakash, J.M. Lattimer, Composition, structure and evolution of neutron stars with kaon condensates, *Nuc. Phys. A* **572**, 693 (1994). [https://doi.org/10.1016/0375-9474\(94\)90407-3](https://doi.org/10.1016/0375-9474(94)90407-3)
- [4] N.K. Glendenning, J. Schaffner-Bielich, Kaon condensation and dynamical nucleons in neutron stars, *Phys. Rev. Lett.* **81**, 4564 (1998). [10.1103/PhysRevLett.81.4564](https://doi.org/10.1103/PhysRevLett.81.4564)
- [5] N. Glendenning, J. Schaffner-Bielich, First order kaon condensate., *Phys. Rev. C* **60**, 025803 (1999). <https://doi.org/10.1103/PhysRevC.60.025803>
- [6] Y. Lim, K. Kwak, C.H. Hyun, C.H. Lee, Kaon condensation in neutron stars with skyrme-hartree-fock models, *Phys. Rev. C* **89**, 055804 (2014). [10.1103/PhysRevC.89.055804](https://doi.org/10.1103/PhysRevC.89.055804)
- [7] D. Kaplan, A. Nelson, Kaon condensation in dense matter., *Nuc. Phys. A* **479**, 273 (1988). [https://doi.org/10.1016/0375-9474\(88\)90442-3](https://doi.org/10.1016/0375-9474(88)90442-3)
- [8] P.S. Koliogiannis, C.C. Moustakidis, Effects of the equation of state on the bulk properties of maximally rotating neutron stars, *Phys. Rev. C* **101**, 015805 (2020). [10.1103/PhysRevC.101.015805](https://doi.org/10.1103/PhysRevC.101.015805)
- [9] V.P. Psonis, C.C. Moustakidis, S.E. Massen, Nuclear symmetry energy effects on neutron stars properties, *Mod. Phys. Lett. A* **22**, 1233 (2007). [10.1142/S0217732307023572](https://doi.org/10.1142/S0217732307023572)
- [10] M.G. Alford, S. Han, M. Prakash, Generic conditions for stable hybrid stars, *Phys. Rev. D* **88**, 083013 (2013). [10.1103/PhysRevD.88.083013](https://doi.org/10.1103/PhysRevD.88.083013)
- [11] B. Abbott et al., Properties of the binary neutron star merger gw170817., *Phys. Rev. X* **9**, 011001 (2019). <https://doi.org/10.1103/PhysRevX.9.011001>
- [12] Z. Arzoumanian et al., The NANOGrav 11-year Data Set: High-precision Timing of 45 Millisecond Pulsars., *Astrophys. J. Suppl. Ser.* **235**, 37 (2018). <https://doi.org/10.3847/1538-4365/aab5b0>
- [13] J. Antoniadis et al., A massive pulsar in a compact relativistic binary., *Science* **340**, 1233232 (2013). <https://doi.org/10.1126/science.1233232>
- [14] H. Cromartie et al., Relativistic Shapiro delay measurements of an extremely massive millisecond pulsar., *Nat. Astron.* **4**, 72 (2020). <https://doi.org/10.1038/s41550-019-0880-2>
- [15] R. Romani, D. Kandel, A. Filippenko, T. Brink, W. Zheng, Sr j0952-0607: The fastest and heaviest known galactic neutron star., *Astrophys. J. Lett.* **934**, L17 (2022). <https://doi.org/10.3847/2041-8213/ac8007>
- [16] V. Doroshenko, V. Suleimanov, G. Pühlhofer, A. Santangelo, A strangely light neutron star within a supernova remnant., *Nat. Astron.* **6**, 1444–1451 (2022). <https://doi.org/10.1038/s41550-022-01800-1>